Superconducting Materials for Microwave Kinetic Inductance Detectors

Benjamin A. Mazin

1.1 Operational Principle

Microwave Kinetic Inductance Detectors, or MKIDs (Day, Leduc, Mazin, et al. 2003; Zmuidzinas 2012), are superconducting resonators suitable for a wide variety of photon and particle detectors. The surface impedance of a superconducting film is complex (Mattis and Bardeen 1958): it has an imaginary part, due to the reactance of the Cooper pairs, that exist together with the familiar geometrical inductance in any superconducting circuit. The real part is due to loss created by quasiparticle excitations, which behave similar to normal electrons. At low temperatures, $T << T_{\rm c}$, the quasiparticle density is exponentially small resulting in a virtually lossless film, even at microwave frequencies.

This extra surface inductance changes when energy (which can come in the form of photons, phonons, or particles) breaks Cooper pairs into quasiparticles. The result is a change in complex surface impedance that depends on the number of Cooper pairs broken by incident photons, making it proportional to the amount of energy deposited in the superconductor. This surface impedance change can be measured by placing a superconducting inductor in a lithographed resonator, as shown in Figure 1. More information on the kinetic inductance effect can be found in Zmuidzinas 2012 and Gao 2008.

A MKID is essentially a microwave LC oscillator with a resonant frequency f_0 in the GHz range. It has nearly perfect transmission away from the resonant frequency, but acts as a short on resonance, much like a high Q notch filter. More information on superconducting resonators can be found in chapter H.2.1.

To read out a MKID a microwave probe signal, typically a simple sine wave, is tuned to the f_0 of the resonator. One photon (in the case of X-ray and optical MKIDs) or many photons (in the case of sub/mm MKIDs) imprint their signature as changes in phase and amplitude of this probe signal. Since the measured quality factor $Q_{\rm m}$ of the resonators is high (usually 10,000–100,000) and the microwave transmission off resonance is almost perfect, multiplexing can be accomplished by tuning each pixel to a different resonant frequency during device fabrication. A comb of probe signals (Figure 2) can be sent into the device, and room temperature electronics can recover the changes in amplitude and phase without significant cross talk (McHugh, Mazin, Serfass, et al. 2012).

The primary advantage over other superconducting detector technologies like transition edge sensors (TESs, Irwin, Hilton, Wollman, and Martinis 1996) is that MKIDs are easy to multiplex, dramatically reducing the number of wires needed to read out an arrays, as shown in Figure 2. They are also typically easier to fabricate than other superconducting sensors in that the usually do not use membranes or micromachining.

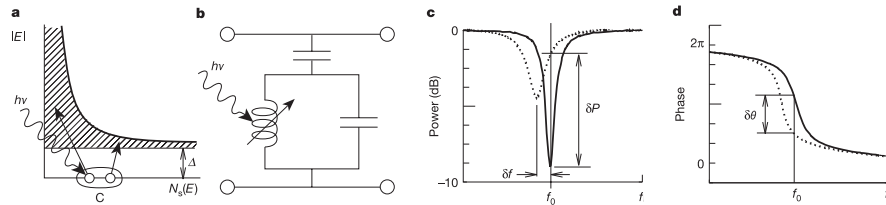While the technology was originally envisioned for sub-mm detectors (Doyle,

1

Figure 1: The basic operational principles of an MKID. (a) Photons with energy $h\nu > 2\Delta$ are absorbed in a superconducting film, producing a number of excitations, called quasiparticles. (b) To sensitively measure these quasiparticles, the film is placed in a high frequency (MHz–GHz) planar resonant circuit. The amplitude (c) and phase (d) of a microwave excitation signal sent through the resonator. The change in the surface impedance of the film following a photon absorption event pushes the resonance to lower frequency and changes its amplitude. If the detector (resonator) is excited with a constant on-resonance microwave signal, the energy of the absorbed photon can be determined by measuring the degree of phase and amplitude shift.

Mauskopf, Naylon, et al. 2008; Calvo, Benoit, Catalano, et al. 2016; Dober, J. A. Austermann, J. A. Beall, et al. 2016; Baselmans, Bueno, Yates, et al. 2017), MKIDs have found applications across the electromagnetic spectrum. X-ray detectors using both non-equilibrium (Mazin, Bumble, Day, et al. 2006) and thermal detection (Ulbricht, Mazin, Szypryt, et al. 2015) have been demonstrated, and significant progress has been made on optical and near-IR arrays for astronomy (Mazin, Bumble, Meeker, et al. 2012; Szypryt, Meeker, Coiffard, et al. 2017). Cosmic Microwave Background (CMB) detectors have also been a focus (Hubmayr, J. Beall, Becker, Cho, Dober, et al. 2013; Matsumura, Akiba, Arnold, et al. 2016; McCarrick, Jones, B. R. Johnson, et al. 2018). Works is also beginning on more serious attempts to use MKIDs for particle detection (Moore, Golwala, Bumble, et al. 2012; Cruciani, Bellini, Cardani, et al. 2016).

1.2 MKID Materials

The superconducting materials that make up an MKID have a significant effect on its performance. The T_c and normal state resistivity ρ_N of the film determine the penetration depth λ and therefore how much kinetic inductance it has (see Zmuidzinas 2012, Section 2.3). The ratio of kinetic inductance to total inductance (α), the volume of the inductor, and Q_m determines the magnitude of the response to incoming energy (see Zmuidzinas 2012, Section 5.3). The quasiparticle lifetime τ_{qp} is the characteristic time during which the MKID's surface impedance is modified by the incoming energy. The response is fairly well understood, but it is only one part of determining the performance of a detector. The noise is the other component, and it is far more complex. The two main source of noise, amplifier noise and two-level system noise, are critically
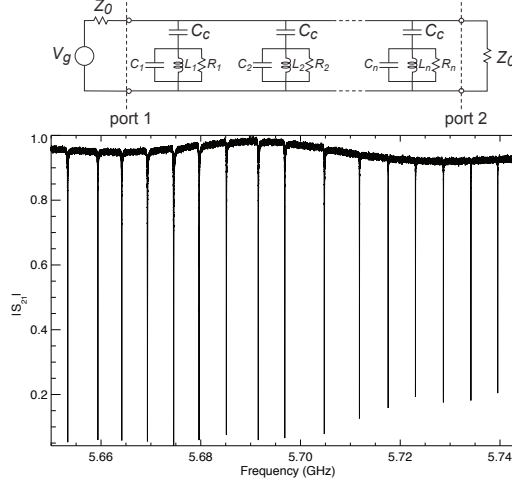
Figure 2: An example of frequency domain multiplexing (FDM) of MKIDs. Each MKID is a superconducting resonator tuned to a different resonant frequency by changing the resonator geometry.

dependent on the maximum microwave readout power that can be used to probe the MKID (see Zmuidzinas 2012, Section 5.4). The exact limits to maximum readout power are thought to be quasiparticle breaking from readout photons in aluminum, and the build up of non-linear kinetic inductance in higher resistivity superconductors. More details can be found in Zmuidzinas 2012, Section 5.7.

Many materials have been explored for use in superconducting resonators and MKIDs, but that information is often not published or scattered around the literature. This chapter contains information and references on the work that has been done with thin film lithographed circuits for MKIDs over the last two decades. Note that measured material properties such as the internal loss quality factor Q_i and quasiparticle lifetime τ_{qp} vary significantly depending on how the MKID superconducting thin film is made and the system they are measured in, so it is best to interpret all stated values as typical but not definitive. Values are omitted in cases when there aren't enough measurements or there is too much disagreement in the literature to estimate a typical value. In order to be as complete as possible some unpublished results from the author's lab are included and can be identified by the lack of a reference. Unless noted all films are polycrystalline or amorphous.

1.2.1 Conventional and High T_c Materials: T_c=4–85 K

High T_c superconductors, for our purposes including conventional high T_c materials and all low T_c materials with transition temperatures from 4 to 85 K, are employed in MKID devices for three reasons. First, they are often used to

construct the microwave transmission lines that bring signals into the arrays because their lower surface impedances tend to make it easier to produce compact 50 Ω feedlines. Second, they are sometimes used as the sensor material in the MKID for applications that have a high incident flux and/or require high temperature operation. This higher temperature operation also reduces cost and complexity of the required cooling system. An example of this kind of application is general purpose terahertz imaging (Rowe, Pascale, Doyle, et al. 2016). Third, long wavelength MKID arrays usually use antennas or transmission lines to deliver the photons to the MKID sensor element. To deliver photon without loss, the superconducting gap of the antenna/transmission line material must be larger than half of the photon energy ($\Delta > h\nu/2$). For example, Nb has a cutoff frequency of 700 GHz while NbTiN can operate to $\sim$1.0 THz.

Superconductor	T_c (K)	Q_i	τ_{qp} (μs)	Notes
YBCO	85	4,000		
MgB$_2$	40	30,000		
NbTiN	15	$> 10^6$	< 1	
MoRe	8–13	7×10^5		Tunable
Nb	9	$> 5 \times 10^5$		
Ta	4.5	$> 10^5$	30	

Table 1: Properties of High T_c MKID Materials. Tunable refers to compound materials whose T_c can be adjusted by varying the stoichiometry.

1.2.1.1 YBCO

There has been limited work using resonators made out of the high T_c superconductor YBCO for MKID work (Lindeman, Bonetti, Bumble, et al. 2014; Chakrabarty, Lindeman, Bumble, et al. 2019), where YCBO forms both the resonator and feedlines. While the measured internal quality factor Q_i is low, on the order of 4,000, it is sufficient for detectors with high incident power, and operation at temperatures above 10 K has been demonstrated.

1.2.1.2 MgB$_2$

Some early work shows that MgB$_2$ is a possible material for MKIDs (Yang, Niu, Guo, et al. 2018). The authors show operation at 7.5 K results in Q_i $\sim$30,000, despite the added complexity of the two-gap material.

1.2.1.3 NbTiN

NbTiN, with a T_c of $\sim$15K, is commonly used as the ground plane material in MKID arrays (Janssen, Baselmans, Endo, et al. 2013). It is a well behaved and well understood material with low loss, and has found applications in similar devices like travelling wave parametric amplifiers (Eom, Day, Leduc, and

Zmuidzinas 2012). Its low loss means that is occasionally used to define the capacitors in a MKID with different materials for the capacitor and the inductor, sometimes called a hybrid MKID.

1.2.1.4 MoRe

Preliminary work on the disordered superconducting alloy MoRe (Singh, Schneider, Bosman, et al. 2014) has shown promising resonator internal quality factors. It has potential applications as both a ground plane and resonator capacitor material, similar to NbTiN.

1.2.1.5 Nb

Nb is perhaps the most commonly used material for MKID ground planes as its elemental nature and wide use makes it almost a requirement in any superconducting fabrication line. Nb is also used for antennas to bring signals to the sensor as well as in passive circuit elements like band-defining filters. Nb resonators tend to have relatively high $Q_i >> 2 \times 10^5$ (Gao, Vale, Mates, et al. 2011; Thakur, Tang, McGeehan, et al. 2017), although deposition conditions (low base pressure during sputtering, stress, and film purity) and substrate appear to play an important role. Advanced Nb fabrication methods developed for superconducting electronics, such as planarization, enable very complex wiring (Devasia, Balvin, Bandler, et al. 2019).

1.2.1.6 Ta

Ta is often used as the absorber in X-ray MKIDs (Mazin, Bumble, Day, et al. 2006) because of its excellent X-ray stopping power due to its high atomic number (73) and density (16.65 g/cm^3). Ta resonators have been fabricated and display similar microwave properties to Nb resonators, although Nb's higher T_{c} means it is used more widely. The quasiparticle lifetime has been measured in several different ways to be approximately 30 μs (Mazin, Bumble, Day, et al. 2006; Barends, Baselmans, Yates, et al. 2008). Most Ta films are polycrystalline, but it has been successfully grown epitaxially by doing a heated deposition on r-plane sapphire. While epi-Ta films have shown residual resistance ratios (RRR) greater than 30, the microwave loss properties appear to be similar to amorphous Ta (Mazin, Bumble, Day, et al. 2006).

1.2.2   Low $T_{\mathbf{C}}$ Materials: $T_c = 0.8 - 4$ K

Low T_{C} superconductors, with transition temperatures from 0.8–4.5 K, are the most common materials used for the sensor element (the inductor of the resonator) in modern MKID arrays. MKIDs are typically operated at $T_{\mathrm{Op}} \leq T_{\mathrm{c}}/8$, so these materials are right in the sweet spot for operation with portable cryogenic technologies like He3 sorption coolers ($T_{\mathrm{Op}} \approx 300$ mK) and adiabatic demagnetization refrigerators (ADRs, $T_{\mathrm{Op}} \approx 100$ mK).

Superconductor	T_c (K)	Q_i	τ_{qp} (μs)	Notes
Re	1.4	$> 4 \times 10^6$		
Al	1.2	$> 10^6$	2000	
Mo	0.9	~ 0		Normal metal oxides
TiN	0.8–4.5	$> 10^7$	50	Tunable
Ti/TiN	0.8–4.5	$> 10^5$		Tunable
WSi$_x$	1.4–4.5	$> 10^6$	<1	Tunable, high heat capacity
PtSi	0.93	$> 5 \times 10^5$	25	Low Q_i on Si

Table 2: Properties of Low T_c MKID Materials.

1.2.2.1   Re

Rhenium (Wang, Hofheinz, Wenner, et al. 2009; Dumur, Delsol, Weissl, et al. 2016) has been explored as an alternative to aluminum, primarily because it has a similar T_c but can be grown epitaxially on a sapphire substrate. Initial efforts showed inferior RF loss performance compared with Al and little effect from epitaxial growth. It has not been pursued much farther because it is less common and more expensive than aluminum.

1.2.2.2   Al

Aluminum was the first MKID material (Day, Leduc, Mazin, et al. 2003), and remains one of the most popular for both sensors and feedlines. Aluminum films are easy to produce, have excellent uniformity, low loss, and long quasiparticle lifetimes. The primary drawback of Al is that its low surface impedance often pushes the user to very thin films, which increases loss and T_c (up to 2 K for the thinnest films) and makes them vulnerable to damage in processing.

Aluminum remains the technology of choice for CMB (McCarrick, Jones, B. R. Johnson, et al. 2018) and sub-mm MKIDs (Janssen, Baselmans, Endo, et al. 2013), and is used widely in lithographed thin film resonators for quantum information experiments (Megrant, Neill, Barends, et al. 2012; Barends, Kelly, Megrant, et al. 2014). It tends not to be used for shorter wavelength detectors where smaller pixels are required.

Significant effort has been spent doping aluminum with mangenese to lower its T_c. This approach works and allows a relatively high Q_i to be maintained (Jones, B. R. Johnson, Abitbol, et al. 2017) down to at least $T_c \sim$ 600 mK, although it has been shown to lower the quasiparticle lifetime (Barends, Baselmans, Yates, et al. 2008).

Recent work has focused on using high resistivity granular aluminum (grAl) for resonators for both MKIDs and qubits (Grünhaupt, Maleeva, Skacel, et al. 2018). It behaves mostly like aluminum but the sheet resistance can be tuned up to at least 4×10^3 $\mu\Omega$ cm, and likely higher as it approaches the superconductor/insulator transition. It is relatively easy to make by depositing aluminum in the presence of oxygen, and is a good candidate when the simplicity of aluminum is helpful but a higher surface impedance per square is required.

1.2.2.3 Mo

Molybdenum resonators seem attractive due to the convenient T_C, but work at JPL failed to produce any working Mo resonators. The most likely scenario is that molybdenum oxides are forming on the surface and remain conductive to low temperatures (Huang, Yao, Sun, et al. 2017). These lossy conductive oxides mean that Mo is likely a material to avoid.

Some success has been had with Mo_2N (Patel, Brown, Hsieh, et al. 2013; Cataldo, Barrentine, Brown, et al. 2016) with $Q_i > 100,000$.

1.2.2.4 TiN_x

Titanium Nitride is an excellent material for MKIDs as it has shown the lowest loss of any known material (Leduc, Bumble, Day, et al. 2010) and has a high normal state resistance which leads to high surface impedance and hence small, sensitive resonators. It has a relatively long quasiparticle life for a disordered superconductor, and the T_C can be tuned over a wide range (0.8–4.5 K) by adjusting the nitrogen content of the film. The T_C drops from stoichiometric TiN (4.5 K) to that of pure Ti (0.4 K) during reactive sputtering of TiN_x, where $x < 1$. However, the extreme sensitivity of T_C to nitrogen content has the effect of making the TiN film spatially non-uniform across the wafer due to process/gas flow imperfections, which shifts resonant frequencies around and lowers yield due to resonator collisions in frequency space. Despite significant effort, low loss substoichiometric TiN_x has only been grown on crystalline silicon substrates, while stoichiometric TiN may give good loss performance on other substrates.

Some groups have had success growing more uniform stoichiometric titanium nitride using atomic layer deposition (Coumou, Zuiddam, Driessen, et al. 2013; Szypryt, Mazin, Bumble, et al. 2015). Successful low loss ALD growth seems to involve making sure the background partial pressure of oxygen is as low as possible. Making sub-stoichiometric TiN_x with lower T_C remains a challenge for ALD.

TiN_x was used in the first generation of optical and near-IR (OIR) MKID arrays (Mazin, Bumble, Meeker, et al. 2012) and X-ray thermal kinetic inductance detectors (TKIDs) (Ulbricht, Mazin, Szypryt, et al. 2015). It is currently being, among other thins, for large area particle detectors (Colantoni, Cardani, Casali, et al. 2018).

1.2.2.5 Ti/TiN Multilayers

Due to the non-uniformity of reactively sputtered TiN a process was developed where alternating layers of Ti and stoichiometric 4.5 K TiN (Vissers, Gao, Sandberg, et al. 2013) were laid down in a superlattice. This leads to dramatically more uniform films, with preliminary measurements of NIST multilayers made at UCSB showing lower Q_i when T_C is pushed below 1 K. It is currently being used in feedhorn-coupled dual polarization submm/far-IR MKID arrays (Hub-
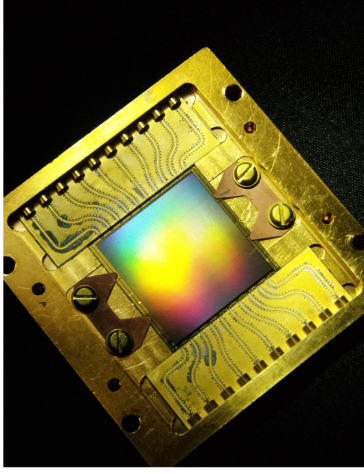
Figure 3: A 20,440 pixel MKID array optimized for near-IR astronomy from Szypryt, Meeker, Coiffard, et al. 2017.

mayr, J. Beall, Becker, Cho, Devlin, et al. 2015; J. E. Austermann, J. A. Beall, Bryan, et al. 2018).

1.2.2.6 WSi$_x$

Tungsten Silicide is an interesting material with a T_c that is tunable by adjusting the W to Si ratio (Kawashima, Muranaka, Kousaka, et al. 2009). It has an extremely short quasiparticle lifetime, which made it interesting for the sensor in a Thermal Kinetic Inductance Detectors (TKIDs) (Cecil, Miceli, Quaranta, et al. 2012). Unfortunately recent work we did at UCSB has shown that WSi grown at UCSB has an anomalously high heat capacity at low temperatures, which degrades TKID performance significantly.

1.2.2.7 PtSi

The non-uniformity issues with TiN caused us to look for another superconducting material that would be stoichiometric at $T_c \sim 900$ mK, very uniform, and would work on an insulating substrate like sapphire. We found this material in platinum silicide (PtSi), and it has led to the highest performance optical and near-IR MKID arrays produced, such as the array chip in a holder shown in Figure 3 (Szypryt, Meeker, Coiffard, et al. 2017). PtSi can be grown by depositing Pt on a Si wafer and doing a thermal anneal, but we observed that this leads to high loss as some Pt atoms diffuse deep into the Si creating a layer of normal metal under the superconducting PtSi (Szypryt, Mazin, Ulbricht, et al. 2016). To avoid this problem and the issues present with OIR detectors on silicon (Marsden, Mazin, Bumble, et al. 2012; Eyken, M. J. Strader, Walter, et al. 2015), we make low loss PtSi by depositing a layer of Si and a layer of Pt on a

sapphire wafer and then doing a thermal anneal at a relatively low temperature (300–400 C).

1.2.3 Very Low $T_{\mathbf{c}}$ Materials: $\mathbf{T}_c < 0.8$ K

The next frontier in MKID sensor materials is going to very low T_{c} materials in order to improve performance. Performance is expected to improve since the signals get larger but the noise does not increase as much. The quasiparticle lifetime $\tau_{\mathrm{qp}} \propto 1/T_{\mathrm{c}}^3$ (Kaplan, Chi, Langenberg, et al. 1976) is also expected to increase. However, care must be taken as microwave losses can increase when the readout frequency becomes a significant fraction of the gap frequency Visser, Goldie, Diener, et al. 2014. This work also requires expensive dilution refrigerators, and significant care must be taken to thermalize the resulting devices.

Superconductor	$T_{\mathbf{c}}$ (K)	$Q_{\mathbf{i}}$	τ_{qp} (μs)	Notes
β-Ta	0.6			
Os	0.66 (0.71-0.77)	8×10^4	120	
Ti	0.40	$< 10^4$		
Hf	0.13 (0.25-0.45)	6×10^5	80	
Ir	0.11			No Oxides

Table 3: Properties of Very Low T_{c} MKID Materials. Measured T_{c} of thin films shown in parenthesis.

1.2.3.1 Ta (β phase)

Under certain conditions tantalum can be grown in the β phase (Schwartz 1972; Colin, Abadias, Michel, and Jaouen 2017), which lowers T_{c} from 4.5 K to approximately 0.6 K. We are not aware of any use of β-Ta for MKIDs, but it remains an intriguing possibility.

1.2.3.2 Os

Osmium is the densest material in the periodic table, and transitions around 0.66 K. It has the fascinating property that it can be etched with oxygen, although the resulting Osmium tetroxide is a highly toxic gas. We have successfully made sputtered Os resonators at UCSB. However, due to concerns about toxicity and stability of devices in the atmosphere we have not pursued it. We measured Q_i =15,000 for ALD Osmium made by Jani Hamalainen in Helsinki, and 80,000 for sputtered Os made at UCSB. We also measured a surprisingly long quasiparticle lifetime of 120 μs in the ALD Osmium devices.

1.2.3.3 Ti

Significant work was done at JPL to produce high quality titanium resonators using UHV sputtering, including using silicon and sapphire substrates, heating
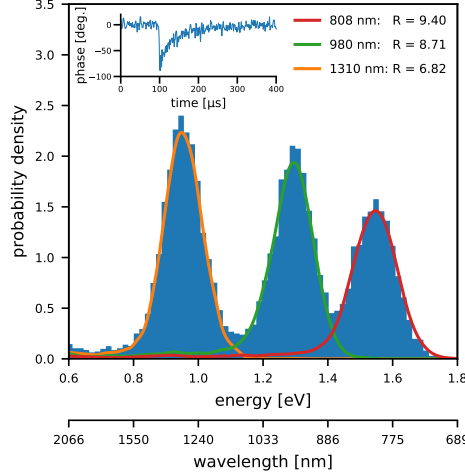
Figure 4: Spectral resolution of a single layer Hf resonator with T_{c}=395 mK, from Zobrist, Coiffard, Bumble, et al. 2019. Ordinate shows the probability of a photon arriving in this bin due to laser illunimation at 808, 980, and 1310 nm. Despite being unoptimized, this Hf MKID is already producing superior energy resolution to PtSi. The poorly fit tail to longer wavelengths is due to the lack of a microlens, which allows photons to impact less sensitive areas of the resonator.

during deposition, and capping the film with a protective superconducting layer to try to prevent oxidation. None of these efforts met with success, with Q_{i} always less than 10,000. Whether this is due to lossy metallic oxides or the Ti gettering impurities during sputtering is unknown.

1.2.3.4   Hf

We have been studying Hf resonators for MKID sensors at UCSB for the last several years (Zobrist, Coiffard, Bumble, et al. 2019; Coiffard, Daal, Zobrist, et al. 2020). The original Hf films we used were deposited at JPL, and more recently at both JPL and UCSB. We have successfully deposited Hf on several different substrates, including high resistivity silicon and r, c, and a-plane sapphire. Initial devices had $T_{\mathrm{c}} \sim 450$ mK, but recent work at JPL has shown that $T_{\mathrm{c}} \sim 200$ mK can be achieved by changing the sputter pressure, as T_{c} appears to depend on film stress. In all cases the thin film T_{c} has been significantly higher than the bulk $T_{\mathrm{c}} = 130$ mK. Q_{i} also appears to depend heavily on film stress with films with high compressive stress showing lower microwave loss. UCSB films with T_{c} =395 mK have a resistivity of 97 $\mu\Omega$ cm. This yields a surface inductance of about 50 pH/sq for a 50 nm thick film, and 20 pH/sq for a 125 nm thick film. Quasiparticle lifetimes in Hf appear to be relatively long, $\sim$80 μs. Despite not being optimized, preliminary Hf MKIDs are already exceeding the spectral resolution of PtSi arrays (Figure 4).

1.2.3.5 Ir

Iridium is a non-reactive metal with a bulk T_C around 112 mK. Due to its non-reactive nature it cannot be etched with conventional reactive ion etches, and must be ion-milled to pattern. JPL has seen resonances in Ir MKIDs, but has not characterized the material properties in a systematic way.

1.3 MKID Instruments and Applications

MKIDs are being used in a variety of astronomical and security applications, with more experiments coming online every year. The following examples are illustrative of what is being done across a wide wavelength range.

1.3.1 Optical/Near-IR

MKID focal planes have so far been incorporated into two main classes of OIR instruments. First, MKIDs have been used in seeing-limited integral field spectrographs (IFSs) for observations of time variable and low surface brightness objects with the ARCONS instrument (Mazin, Meeker, M. J. Strader, et al. 2013) at the Palomar 200" telescope. This testbed instrument led to a number of interesting scientific results (M. J. Strader, M. D. Johnson, Mazin, et al. 2013; Szypryt, Duggan, Mazin, et al. 2014; M. J. Strader, Archibald, Meeker, et al. 2016; Collura, P. Strader, Meeker, et al. 2017), but a true facility class instrument is needed to make further progress.

The second class of IFSs using MKIDs have been for high contrast direct imaging of exoplanets behind adaptive optics systems and a coronagraph. For this application the near-IR sensitivity, lack of read noise, and fast readout enable active speckle suppression (Martinache, Guyon, Jovanovic, et al. 2014) as well as extremely effective time-based speckle suppression using stochastic speckle discrimination (Walter, Bockstiegel, Brandt, and Mazin 2019). Existing MKID instruments for this application include DARKNESS for the Palomar 200" (Meeker, Mazin, Walter, et al. 2018), MEC for Subaru SCExAO, and the PICTURE-C NASA balloon mission which is under construction.

1.3.2 Sub-mm/CMB

The MUSIC (Sayers, Bockstiegel, Brugger, et al. 2014), NIKA (Monfardini, Swenson, Bideaud, et al. 2010), and NIKA2 (Adam, Adane, Ade, et al. 2018) instruments were some of the first instruments to use large arrays of MKIDs for mapping the sky in the sub-mm and mm wavelength. DESHIMA (Endo, Karatsu, Laguna, et al. 2019) is novel sub-mm spectrometer using an on-chip filter bank spectrometer coupled to a MKID array. It has recently been fielded at the ASTE telescope in Chile and returned its first astronomical results, included the detection of redshifted C[IV] emission from dusty star-forming galaxies (Endo, Karatsu, Tamura, et al. 2019). Future iterations of DESHIMA and

the similar instrument SUPERSPEC (Wheeler, Hailey-Dunsheath, Shirokoff, et al. 2018) will be powerful tools for investigating the high redshift universe.

1.3.3 THz

Airport security cameras can look though clothes and detect hidden objects. A joint venture is building THz MKIDs designed for passive THz video imaging to faster and less intrusive airport screening (Rowe, Pascale, Doyle, et al. 2016).

1.4 Discussion

MKIDs are very flexible devices, but unfortunately new thin film MKID materials tend to be approached in a trial and error fashion due to the complexity of the possible outcomes and the large parameter space that must be explored, including deposition method (sputtering, e-beam or thermal evaporation, laser ablation, chemical vapor deposition, etc.), temperature, pressure, rate, and substrate. Despite these challenges many suitable MKID materials have been discovered, allowing detector designers to chose materials most suitable for a given application. In the coming years more materials will be explored, especially in the very low T_c regime, paving the way for MKIDs of unprecedented sensitivity.

References

Adam, R., Adane, A., Ade, P. A. R., André, P., Andrianasolo, A., Aussel, H., Beelen, A., Benoit, A., Bideaud, A., Billot, N., Bourrion, O., Bracco, A., Calvo, M., Catalano, A., Coiffard, G., Comis, B., De Petris, M., Désert, F. X., Doyle, S., Driessen, E. F., Evans, R., Goupy, J., Kramer, C., Lagache, G., Leclercq, S., Leggeri, J. P., Lestrade, J. F., Macias-Perez, J. F., Mauskopf, P., Mayet, F., Maury, A., Monfardini, A., Navarro, S., Pascale, E., Perotto, L., Pisano, G., Ponthieu, N., Revéret, V., Rigby, A., Ritacco, A., Romero, C., Roussel, H., Ruppin, F., Schuster, K., Sievers, A., Triqueneaux, S., Tucker, C., and Zylka, R. (2018) The NIKA2 large-field-of-view millimetre continuum camera for the 30 m IRAM telescope. Astronomy and Astrophysics, 609:A115.

Austermann, J. E., Beall, J. A., Bryan, S. A., Dober, B., Gao, J., Hilton, G., Hubmayr, J., Mauskopf, P., McKenney, C. M., Simon, S. M., Ullom, J. N., Vissers, M. R., and Wilson, G. W. (2018) Millimeter-Wave Polarimeters Using Kinetic Inductance Detectors for TolTEC and Beyond. Journal of Low Temperature Physics, 193 (3):120–127.

Barends, R., Baselmans, J. J., Yates, S. J., Gao, J. R., Hovenier, J. N., and Klapwijk, T. M. (2008) Quasiparticle Relaxation in Optically Excited High-Q Superconducting Resonators. Physical Review Letters, 100 (2):257002.

Barends, R., Kelly, J., Megrant, A., Veitia, A., Sank, D., Jeffrey, E., White, T. C., Mutus, J., Fowler, A. G., Campbell, B., Chen, Y., Chen, Z., Chiaro, B., Dunsworth, A., Neill, C., O'Malley, P., Roushan, P., Vainsencher, A., Wenner, J., Korotkov, A. N., Cleland, A. N., and Martinis, J. M. (2014) Superconducting quantum circuits at the surface code threshold for fault tolerance. Nature, 508 (7):500–503.

Baselmans, J. J., Bueno, J., Yates, S. J., Yurduseven, O., Llombart, N., Karatsu, K., Baryshev, A. M., Ferrari, L., Endo, A., Thoen, D. J., Visser, P. J. de, Janssen, R. M. J., Murugesan, V., Driessen, E. F., Coiffard, G., Martin-Pintado, J., Hargrave, P., and Griffin, M. (2017) A kilo-pixel imaging system for future space based far-infrared observatories using microwave kinetic inductance detectors. Astronomy and Astrophysics, 601:A89.

Calvo, M., Benoit, A., Catalano, A., Goupy, J., Monfardini, A., Ponthieu, N., Barria, E., Bres, G., Grollier, M., Garde, G., Leggeri, J. P., Pont, G., Triqueneaux, S., Adam, R., Bourrion, O., Macias-Perez, J. F., Rebolo, M., Ritacco, A., Scordilis, J. P., Tourres, D., Adane, A., Coiffard, G., Leclercq, S., Désert, F. X., Doyle, S., Mauskopf, P., Tucker, C., Ade, P., André, P., Beelen, A., Belier, B., Bideaud, A., Billot, N., Comis, B., D'Addabbo, A., Kramer, C., Martino, J., Mayet, F., Pajot, F., Pascale, E., Perotto, L., Revéret, V., Rodriguez, L., Savini, G., Schuster, K., Sievers, A., and Zylka, R. (2016) The NIKA2 Instrument, A Dual-Band Kilopixel KID Array for Millimetric Astronomy. Journal of Low Temperature Physics, 184 (3):816–823.

Cataldo, G., Barrentine, E. M., Brown, A., Moseley, S. H., U-yen, K., and Wollack, E. J. (2016) Fabrication and Characterization of Superconducting Resonators. Jove-Journal of Visualized Experiments, (111).

Cecil, T., Miceli, A., Quaranta, O., Liu, C., Rosenmann, D., McHugh, S., and Mazin, B. (2012) Tungsten silicide films for microwave kinetic inductance detectors. 101 (3):032601.

Chakrabarty, A., Lindeman, M. A., Bumble, B., Kleinsasser, A. W., Holmes, W. A., and Cunnane, D. (2019) Operation of YBCO kinetic-inductance bolometers for outer solar system missions. Applied Physics Letters, 114 (1):132601.

Coiffard, G., Daal, M., Zobrist, N., Swimmer, N., Steiger, S., Bumble, B., and Mazin, B. A. (2020) Characterization of sputtered hafnium thin films for high quality factor microwave kinetic inductance detectors. arXiv.org:arXiv:2004.00736. arXiv: 2004.00736 [2004].

Colantoni, I., Cardani, L., Casali, N., Cruciani, A., Bellini, F., Castellano, M. G., Cosmelli, C., D'Addabbo, A., Di Domizio, S., Martinez, M., Tomei, C., and Vignati, M. (2018) Design and Fabrication of the Second-Generation KID-Based Light Detectors of CALDER. Journal of Low Temperature Physics, 193 (5):726–731.

Colin, J. J., Abadias, G., Michel, A., and Jaouen, C. (2017) On the origin of the metastable beta-Ta phase stabilization in tantalum sputtered thin films. Acta Materialia, 126:481–493.

Collura, G., Strader, P., Meeker, S. R., Szypryt, P., Walter, A. B., Bockstiegel, C., Mazin, B. A., and Prince, T. A. (2017) Search for Optical Pulsation in M82 X-2. The Astrophysical Journal, 850 (1):65.

Coumou, P., Zuiddam, M. R., Driessen, E. F., Visser, P. J. de, Baselmans, J. J., and Klapwijk, T. M. (2013) Microwave Properties of Superconducting Atomic-Layer Deposited TiN Films. Ieee Transactions on Applied Superconductivity, 23:7500404–7500404.

Cruciani, A., Bellini, F., Cardani, L., Casali, N., Castellano, M. G., Colantoni, I., Coppolecchia, A., Cosmelli, C., D'Addabbo, A., Di Domizio, S., Martinez, M., Tomei, C., and Vignati, M. (2016) Phonon-Mediated KIDs as Light Detectors for Rare-Event Search: The CALDER Project. Journal of Low Temperature Physics, 184 (3-4):859–865.

Day, P. K., Leduc, H. G., Mazin, B. A., Vayonakis, A., and Zmuidzinas, J. (2003) A broadband superconducting detector suitable for use in large arrays. Nature, 425 (6):817–821.

Devasia, A. M., Balvin, M. A., Bandler, S. R., Bolkhovsky, V., Nagler, P. C., Ryu, K., Smith, S. J., Stevenson, T. R., and Yoon, W. (2019) Fabrication of Magnetic Calorimeter Arrays With Buried Wiring. Ieee Transactions on Applied Superconductivity, 29 (5):2902530–6.

Dober, B., Austermann, J. A., Beall, J. A., Becker, D., Che, G., Cho, H., Devlin, M., Duff, S. M., Galitzki, N., Gao, J., Groppi, C., Hilton, G. C., Hubmayr, J., Irwin, K. D., McKenney, C. M., Li, D., Lourie, N., Mauskopf, P., Vissers, M. R., and Wang, Y. (2016) Optical Demonstration of THz, Dual-Polarization Sensitive Microwave Kinetic Inductance Detectors. Journal of Low Temperature Physics, 184 (1-2):173–179.

Doyle, S., Mauskopf, P., Naylon, J., Porch, A., and Duncombe, C. (2008) Lumped element kinetic inductance detectors. Journal of Low Temperature Physics, 151 (1-2):530–536.

Dumur, E., Delsol, B., Weissl, T., Kung, B., Guichard, W., Hoarau, C., Naud, C., Hasselbach, K., Buisson, O., Ratter, K., and Gilles, B. (2016) Epitaxial Rhenium Microwave Resonators. Ieee Transactions on Applied Superconductivity, 26 (3):–4.

Endo, A., Karatsu, K., Laguna, A. P., Mirzaei, B., Huiting, R., Thoen, D. J., Murugesan, V., Yates, S. J. C., Bueno, J., Marrewijk, N. v., Bosma, S., Yurduseven, O., Llombart, N., Suzuki, J., Naruse, M., Visser, P. J. de, Werf, P. P. van der, Klapwijk, T. M., and Baselmans, J. J. A. (2019) Wideband on-chip terahertz spectrometer based on a superconducting filterbank. Journal of Astronomical Telescopes, 5 (3):035004.

Endo, A., Karatsu, K., Tamura, Y., Oshima, T., Taniguchi, A., Takekoshi, T., Asayama, S., Bakx, T. J., Bosma, S., Bueno, J., Chin, K. W., Fujii, Y., Fujita, K., Huiting, R., Ikarashi, S., Ishida, T., Ishii, S., Kawabe, R., Klapwijk, T. M., Kohno, K., Kouchi, A., Llombart, N., Maekawa, J., Murugesan, V., Nakatsubo, S., Naruse, M., Ohtawara, K., Pascual Laguna, A., Suzuki, J., Suzuki, K., Thoen, D. J., Tsukagoshi, T., Ueda, T., Visser, P. J. de, Werf, P. P. van der, Yates, S. J. C., Yoshimura, Y., Yurduseven, O., and Baselmans,

J. J. A. (2019) First light demonstration of the integrated superconducting spectrometer. Nature Astronomy:1–8.

Eom, B. H., Day, P. K., Leduc, H. G., and Zmuidzinas, J. (2012) A wideband, low-noise superconducting amplifier with high dynamic range. Nature Physics, 8 (8):623–627.

Eyken, J. C. van, Strader, M. J., Walter, A. B., Meeker, S. R., Szypryt, P., Stoughton, C., O'Brien, K., Marsden, D., Rice, N. K., Lin, Y., and Mazin, B. A. (2015) The Arcons Pipeline: Data Reduction for Mkid Arrays. Astrophysical Journal Supplement Series, 219 (1).

Gao, J. (2008) The physics of superconducting microwave resonators. PhD thesis, California Institute of Technology, Pasadena, CA.

Gao, J., Vale, L. R., Mates, J. A. B., Schmidt, D. R., Hilton, G. C., Irwin, K. D., Mallet, F., Castellanos-Beltran, M. A., Lehnert, K. W., Zmuidzinas, J., and LeDuc, H. G. (2011) Strongly quadrature-dependent noise in superconducting microresonators measured at the vacuum-noise limit. Applied Physics Letters, 98 (23).

Grünhaupt, L., Maleeva, N., Skacel, S. T., Calvo, M., Levy-Bertrand, F., Ustinov, A. V., Rotzinger, H., Monfardini, A., Catelani, G., and Pop, I. M. (2018) Loss Mechanisms and Quasiparticle Dynamics in Superconducting Microwave Resonators Made of Thin-Film Granular Aluminum. Physical Review Letters, 121 (1):117001.

Huang, L., Yao, B., Sun, J., Gao, X., Wu, J., Wan, J., Li, T., Hu, Z., and Zhou, J. (2017) Highly conductive and flexible molybdenum oxide nanopaper for high volumetric supercapacitor electrode. Journal of Materials Chemistry A, 5 (6):2897–2903.

Hubmayr, J., Beall, J., Becker, D., Cho, H., Devlin, M., Dober, B., Groppi, C., Hilton, G. C., Irwin, K. D., Li, D., Mauskopf, P., Pappas, D. P., Van Lanen, J., Vissers, M. R., Wang, Y., Wei, L. F., and Gao, J. (2015) Photon-noise limited sensitivity in titanium nitride kinetic inductance detectors. Applied Physics Letters, 106 (7):073505.

Hubmayr, J., Beall, J., Becker, D., Cho, H., Dober, B., Devlin, M., Fox, A. M., Gao, J., Hilton, G. C., Irwin, K. D., Li, D., Niemack, M. D., Pappas, D. P., Vale, L., and Vissers, M. (2013) Dual-Polarization Sensitive MKIDs for Far Infrared Astrophysics. Ieee Transactions on Applied Superconductivity, 23 (3):2400304.

Irwin, K., Hilton, G., Wollman, D., and Martinis, J. (1996) X-ray detection using a superconducting transition-edge sensor microcalorimeter with electrothermal feedback. 69 (13):1945–1947.

Janssen, R. M. J., Baselmans, J. J., Endo, A., Ferrari, L., Yates, S. J., Baryshev, A. M., and Klapwijk, T. M. (2013) High optical efficiency and photon noise limited sensitivity of microwave kinetic inductance detectors using phase readout. Applied Physics Letters, 103 (20).

Jones, G., Johnson, B. R., Abitbol, M. H., Ade, P. A. R., Bryan, S., Cho, H., Day, P., Flanigan, D., Irwin, K. D., Li, D., Mauskopf, P., McCarrick, H., Miller, A., Song, Y. R., and Tucker, C. (2017) High quality factor manganese-

doped aluminum lumped-element kinetic inductance detectors sensitive to frequencies below 100 GHz. Applied Physics Letters, 110 (2):222601.

Kaplan, S., Chi, C., Langenberg, D., Chang, J., Jafarey, S., and Scalapino, D. (1976) Quasiparticle Lifetimes in Superconductors. Bulletin Of The American Physical Society, 21 (3):258–259.

Kawashima, K., Muranaka, T., Kousaka, Y., Akutagawa, S., and Akimitsu, J. (2009) Superconductivity in transition metal-silicide W5Si3. Journal of Physics: Conference Series, 150 (5):052106.

Leduc, H. G., Bumble, B., Day, P. K., Eom, B. H., Gao, J., Golwala, S., Mazin, B. A., McHugh, S., Merrill, A., Moore, D. C., Noroozian, O., Turner, A. D., and Zmuidzinas, J. (2010) Titanium nitride films for ultrasensitive microresonator detectors. Applied Physics Letters, 97 (1):2509.

Lindeman, M. A., Bonetti, J. A., Bumble, B., Day, P. K., Eom, B.-H., Holmes, W. A., and Kleinsasser, A. W. (2014) Arrays of membrane isolated yttrium-barium-copper-oxide kinetic inductance bolometers. Journal Of Applied Physics, 115 (23).

Marsden, D., Mazin, B. A., Bumble, B., Meeker, S., O'Brien, K., McHugh, S., Strader, M., and Langman, E. (2012) Optical lumped element microwave kinetic inductance detectors. Proceedings of SPIE, 8453.

Martinache, F., Guyon, O., Jovanovic, N., Clergeon, C., Singh, G., Kudo, T., Currie, T., Thalmann, C., McElwain, M., and Tamura, M. (2014) On-Sky Speckle Nulling Demonstration at Small Angular Separation with SCExAO. Publications of the Astronomical Society of the Pacific, 126 (940):565–572.

Matsumura, T., Akiba, Y., Arnold, K., et al. (2016) LiteBIRD: Mission Overview and Focal Plane Layout. Journal of Low Temperature Physics, 184 (3-4):824–831.

Mattis, D. C. and Bardeen, J. (1958) Theory of the Anomalous Skin Effect in Normal and Superconducting Metals. Physical Review, 111 (2):412–417.

Mazin, B. A., Meeker, S. R., Strader, M. J., Szypryt, P., Marsden, D., Eyken, J. C. van, Duggan, G. E., Walter, A. B., Ulbricht, G., Johnson, M., Bumble, B., O'Brien, K., and Stoughton, C. (2013) ARCONS: A 2024 Pixel Optical through Near-IR Cryogenic Imaging Spectrophotometer. Publications of the Astronomical Society of the Pacific, 125:1348–1361.

Mazin, B. A., Bumble, B., Day, P. K., Eckart, M. E., Golwala, S., Zmuidzinas, J., and Harrison, F. A. (2006) Position sensitive x-ray spectrophotometer using microwave kinetic inductance detectors. Applied Physics Letters, 89 (2):2507.

Mazin, B. A., Bumble, B., Meeker, S. R., O'Brien, K., McHugh, S., and Langman, E. (2012) A superconducting focal plane array for ultraviolet, optical, and near-infrared astrophysics. Optics Express, 20 (2):1503–1511.

McCarrick, H., Jones, G., Johnson, B. R., Abitbol, M. H., Ade, P. A. R., Bryan, S., Day, P., Essinger-Hileman, T., Flanigan, D., LeDuc, H. G., Limon, M., Mauskopf, P., Miller, A., and Tucker, C. (2018) Design and performance of dual-polarization lumped-element kinetic inductance detectors for millimeter-wave polarimetry. Astronomy and Astrophysics, 610:A45.

McHugh, S., Mazin, B. A., Serfass, B., Meeker, S., O'Brien, K., Duan, R., Raffanti, R., and Werthimer, D. (2012) A readout for large arrays of microwave kinetic inductance detectors. Review of Scientific Instruments, 83 (4):4702.

Meeker, S. R., Mazin, B. A., Walter, A. B., Strader, P., Fruitwala, N., Bockstiegel, C., Szypryt, P., Ulbricht, G., Coiffard, G., Bumble, B., Cancelo, G., Zmuda, T., Treptow, K., Wilcer, N., Collura, G., Dodkins, R., Lipartito, I., Zobrist, N., Bottom, M., Shelton, J. C., Mawet, D., Eyken, J. C. van, Vasisht, G., and Serabyn, E. (2018) DARKNESS: A Microwave Kinetic Inductance Detector Integral Field Spectrograph for High-contrast Astronomy. Publications of the Astronomical Society of the Pacific, 130 (9):065001–.

Megrant, A., Neill, C., Barends, R., Chiaro, B., Chen, Y., Feigl, L., Kelly, J., Lucero, E., Mariantoni, M., O'Malley, P. J. J., Sank, D., Vainsencher, A., Wenner, J., White, T. C., Yin, Y., Zhao, J., Palmstrom, C. J., Martinis, J. M., and Cleland, A. N. (2012) Planar superconducting resonators with internal quality factors above one million. Applied Physics Letters, 100 (11).

Monfardini, A., Swenson, L. J., Bideaud, A., Désert, F. X., Yates, S. J., Benoit, A., Baryshev, A. M., Baselmans, J. J., Doyle, S., Klein, B., Roesch, M., Tucker, C., Ade, P., Calvo, M., Camus, P., Giordano, C., Guesten, R., Hoffmann, C., Leclercq, S., Mauskopf, P., and Schuster, K. F. (2010) NIKA: A millimeter-wave kinetic inductance camera. Astronomy and Astrophysics, 521:29.

Moore, D. C., Golwala, S. R., Bumble, B., Cornell, B., Day, P. K., LeDuc, H. G., and Zmuidzinas, J. (2012) Position and energy-resolved particle detection using phonon-mediated microwave kinetic inductance detectors. Applied Physics Letters, 100 (23):232601.

Patel, A., Brown, A., Hsieh, W., Stevenson, T., Moseley, S. H., U-yen, K., Ehsan, N., Barrentine, E., Manos, G., and Wollack, E. J. (2013) Fabrication of MKIDS for the MicroSpec Spectrometer. Ieee Transactions on Applied Superconductivity, 23 (3):2400404–2400404.

Rowe, S., Pascale, E., Doyle, S., Dunscombe, C., Hargrave, P., Papageorgio, A., Wood, K., Ade, P. A. R., Barry, P., Bideaud, A., Brien, T., Dodd, C., Grainger, W., House, J., Mauskopf, P., Moseley, P., Spencer, L., Sudiwala, R., Tucker, C., and Walker, I. (2016) A passive terahertz video camera based on lumped element kinetic inductance detectors. Review of Scientific Instruments, 87 (3):033105.

Sayers, J., Bockstiegel, C., Brugger, S., Czakon, N. G., Day, P. K., Downes, T. P., Duan, R. P., Gao, J., Gill, A. K., Glenn, J., Golwala, S. R., Hollister, M. I., Lam, A., Leduc, H. G., Maloney, P. R., Mazin, B. A., McHugh, S. G., Miller, D. A., Mroczkowski, A. K., Noroozian, O., Nguyen, H. T., Schlaerth, J. A., Siegel, S. R., Vayonakis, A., Wilson, P. R., and Zmuidzinas, J. (2014) The status of MUSIC: the multiwavelength sub-millimeter inductance camera. *Proceedings of the SPIE*. California Institute of Technology (United States). International Society for Optics and Photonics, 915304.

Schwartz, N. (1972) Temperature coefficient of resistance of beta-tantalum films and mixtures with b.c.c.-tantalum. Thin Solid Films, 14:333–346.

Singh, V., Schneider, B. H., Bosman, S. J., Merkx, E. P. J., and Steele, G. A. (2014) Molybdenum-rhenium alloy based high-Q superconducting microwave resonators. Applied Physics Letters, 105 (22).

Strader, M. J., Archibald, A. M., Meeker, S. R., Szypryt, P., Walter, A. B., Eyken, J. C. van, Ulbricht, G., Stoughton, C., Bumble, B., Kaplan, D. L., and Mazin, B. A. (2016) Search for optical pulsations in PSR J0337+1715. Monthly Notices of the Royal Astronomical Society, 459 (1):427–430.

Strader, M. J., Johnson, M. D., Mazin, B. A., Spiro Jaeger, G. V., Gwinn, C. R., Meeker, S. R., Szypryt, P., Eyken, J. C. van, Marsden, D., O'Brien, K., Walter, A. B., Ulbricht, G., Stoughton, C., and Bumble, B. (2013) Excess Optical Enhancement Observed with ARCONS for Early Crab Giant Pulses. The Astrophysical Journal Letters, 779 (1):L12.

Szypryt, P., Duggan, G. E., Mazin, B. A., Meeker, S. R., Strader, M. J., Eyken, J. C. van, Marsden, D., O'Brien, K., Walter, A. B., Ulbricht, G., Prince, T. A., Stoughton, C., and Bumble, B. (2014) Direct detection of SDSS J0926+3624 orbital expansion with ARCONS. Monthly Notices of the Royal Astronomical Society, 439 (3):2765–2770.

Szypryt, P., Mazin, B. A., Ulbricht, G., Bumble, B., Meeker, S. R., Bockstiegel, C., and Walter, A. B. (2016) High quality factor platinum silicide microwave kinetic inductance detectors. Applied Physics Letters, 109 (15).

Szypryt, P., Meeker, S. R., Coiffard, G., Fruitwala, N., Bumble, B., Ulbricht, G., Walter, A. B., Daal, M., Bockstiegel, C., Collura, G., Zobrist, N., Lipartito, I., and Mazin, B. A. (2017) Large-format platinum silicide microwave kinetic inductance detectors for optical to near-IR astronomy. Optics Express, 25 (21):25894–25909.

Szypryt, P., Mazin, B. A., Bumble, B., LeDuc, H. G., and Baker, L. (2015) Ultraviolet, Optical, and Near-IR Microwave Kinetic Inductance Detector Materials Developments. 25 (3).

Thakur, R. B., Tang, Q. Y., McGeehan, R., Carter, F., and Shirokoff, E. (2017) Characterizing Quality Factor of Niobium Resonators Using a Markov Chain Monte Carlo Approach. Ieee Transactions on Applied Superconductivity, 27 (4).

Ulbricht, G., Mazin, B. A., Szypryt, P., Walter, A. B., Bockstiegel, C., and Bumble, B. (2015) Highly multiplexible thermal kinetic inductance detectors for x-ray imaging spectroscopy. Applied Physics Letters, 106 (25):251103.

Visser, P. J. de, Goldie, D. J., Diener, P., Withington, S., Baselmans, J. J., and Klapwijk, T. M. (2014) Evidence of a Nonequilibrium Distribution of Quasiparticles in the Microwave Response of a Superconducting Aluminum Resonator. Physical Review Letters, 112 (4):047004.

Vissers, M. R., Gao, J., Sandberg, M., Duff, S. M., Wisbey, D. S., Irwin, K. D., and Pappas, D. P. (2013) Proximity-coupled Ti/TiN multilayers for use in kinetic inductance detectors. 102 (23).

Walter, A. B., Bockstiegel, C., Brandt, T. D., and Mazin, B. A. (2019) Stochastic Speckle Discrimination with Time-Tagged Photon Lists: Digging Below the Speckle Noise Floor. Publications of the Astronomy Society of the Pacific, 131 (1005):114506.

Wang, H., Hofheinz, M., Wenner, J., Ansmann, M., Bialczak, R. C., Lenander, M., Lucero, E., Neeley, M., O'Connell, A. D., Sank, D., Weides, M., Cleland, A. N., and Martinis, J. M. (2009) Improving the coherence time of superconducting coplanar resonators. Applied Physics Letters, 95 (23).

Wheeler, J., Hailey-Dunsheath, S., Shirokoff, E., Barry, P. S., Bradford, C. M., Chapman, S., Che, G., Doyle, S., Glenn, J., Gordon, S., Hollister, M., Kovacs, A., LeDuc, H. G., Mauskopf, P., McGeehan, R., McKenney, C., Reck, T., Redford, J., Ross, C., Shiu, C., Tucker, C., Turner, J., Walker, S., and Zmuidzinas, J. (2018) SuperSpec, The On-Chip Spectrometer: Improved NEP and Antenna Performance. Journal of Low Temperature Physics, 193 (3-4):408–414.

Yang, C., Niu, R. R., Guo, Z. S., Cai, X. W., Chu, H. M., Yang, K., Wang, Y., Feng, Q. R., and Gan, Z. Z. (2018) Lumped element kinetic inductance detectors based on two-gap MgB2 thin films. Applied Physics Letters, 112 (2).

Zmuidzinas, J. (2012) Superconducting Microresonators: Physics and Applications. Annual Review of Condensed Matter Physics, 3:169–214.

Zobrist, N., Coiffard, G., Bumble, B., Swimmer, N., Steiger, S., Daal, M., Collura, G., Walter, A. B., Bockstiegel, C., Fruitwala, N., Lipartito, I., and Mazin, B. A. (2019) Design and performance of hafnium optical and near-IR kinetic inductance detectors. Applied Physics Letters, 115 (2):213503.